Mars 2025

BLEFCO

Biologistes des Laboratoires d'Etude de la Fécondation et de la Conservation de l'Oeuf

Automatisation de la Sélection des Spermatozoïdes avant ICSI

Nino Guy Cassuto Labo Drouot Paris

Journée des Techniciens et Biologistes en AMP

National Library of Medicine
National Center for Biotechnology Information

Log in

PubMed®

Human Sperm Selection

Search

Advanced Create alert Create RSS User Guide

Save Email Send to Sort by: Most recent Display options

MY CUSTOM FILTERS

6,429 Results

Page 1 of 643

RESULTS BY YEAR

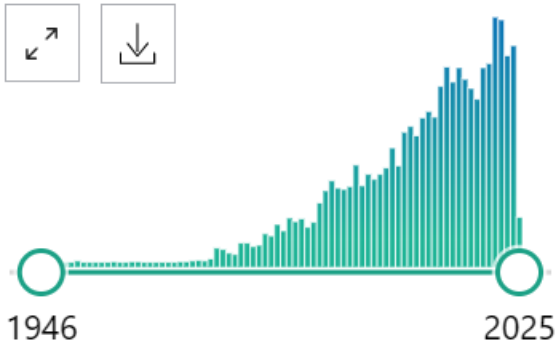

PUBLICATION DATE

1

Cite

Share

The major phytocannabinoids, delta-9-tetrahydrocannabinol (THC) and cannabidiol (CBD), affect the function of CatSper calcium channels in **human sperm**.

Wehrli L, Altevogt H, Brenker C, Zufferey F, Rossier MF, Strünker T, Nef S, Rahban R.

Hum Reprod. 2025 Mar 12:deaf020. doi: 10.1093/humrep/deaf020. Online ahead of print.

PMID: 40078063

STUDY QUESTION: Do the main psychoactive phytocannabinoid delta-9-tetrahydrocannabinol (THC) and its non-psychoactive analog cannabidiol (CBD) affect **human sperm** function? SUMMARY ANSWER: THC and CBD affect the **sperm**-specific Ca2+ channel CatSper, suppress ac ...

National Library of Medicine
National Center for Biotechnology Information

Log in

PubMed®

Human Sperm Selection; artificial intelligence

Search

Advanced Create alert Create RSS User Guide

Save Email Send to Sort by: Most recent Display options

MY CUSTOM FILTERS

81 Results

Page 1 of 9

RESULTS BY YEAR

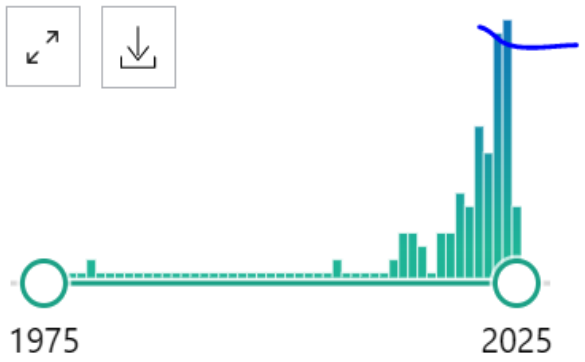

1 Cite Share

A Narrative Review on the **Sperm Selection** Methods in Assisted Reproductive Technology: Out with the New, the Old Is Better?

Tiptiri-Kourpeti A, Asimakopoulos B, Nikolettos N.

J Clin Med. 2025 Feb 7;14(4):1066. doi: 10.3390/jcm14041066.

PMID: 40004597 Free PMC article. Review.

Advanced methods like magnetic-activated cell sorting (MACS) and microfluidic sorting have emerged as more precise tools for **selecting sperm** with better **genetic** integrity, although they face challenges in terms of their standardization, cost, and clinical ado ...

Total Fertility Rate TFR, globally and by Global Burden of Diseases GBD 1950 – 2100

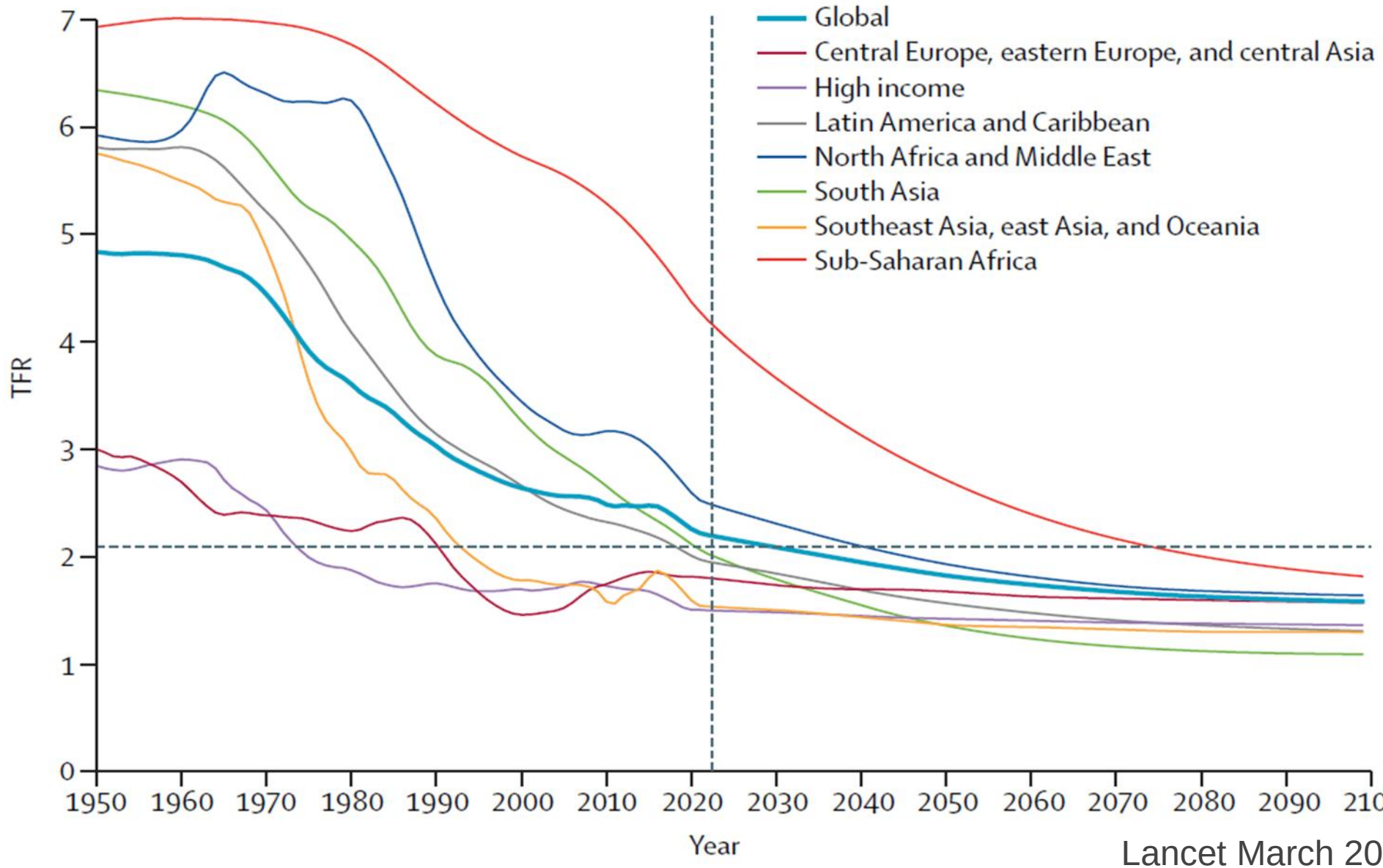

Lancet March 2024

Spermatozoa over the time

1951	100 Millions/ ml
1970	90 Millions/ ml
1974	75 Millions/ ml
1998	55 Millions/ ml
2005	51 Millions/ ml

50 Millions / ml decrease in 50 years

Human Reproduction Update November 2017

Potential effects of exposure to environmental factors on declining fertility rates

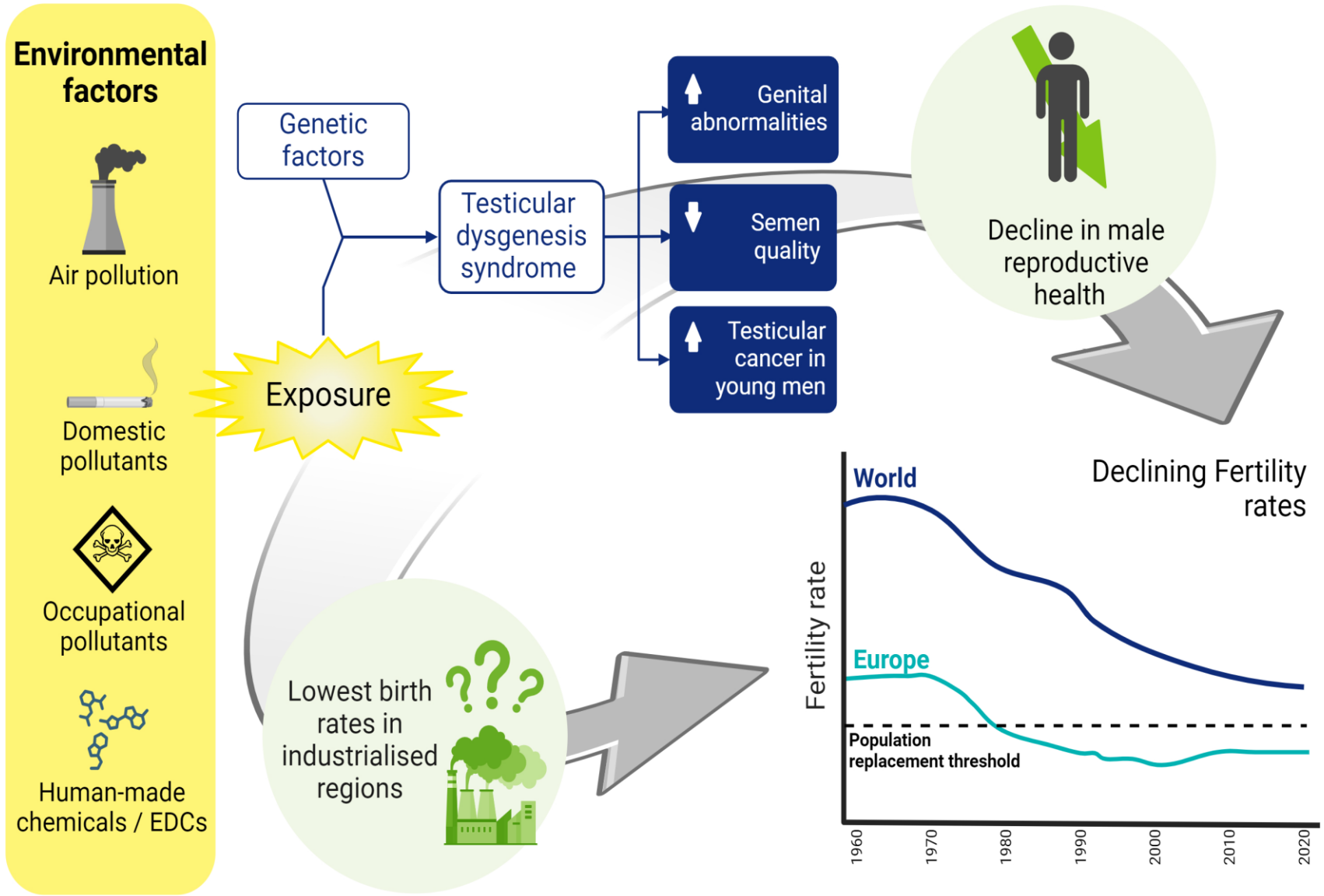

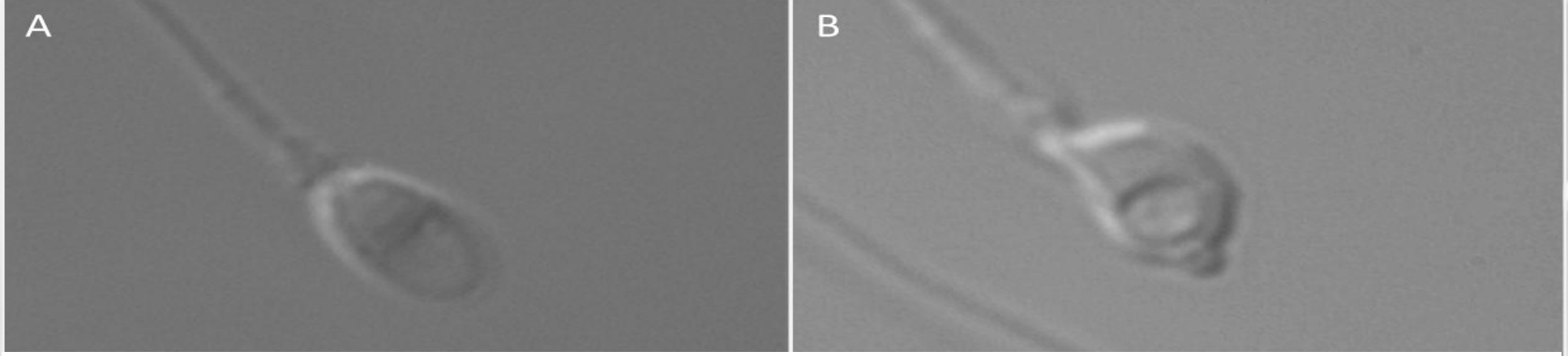

A new real-time morphology classification for human spermatozoa: a link for fertilization and improved embryo quality

Nino Guy Cassuto, M.D.,[a] Dominique Bouret, M.D.,[a] Jean Michel Plouchart, M.D.,[a] Sonia Jellad, M.D.,[a] Pierre Vanderzwalmen, M.S.,[a] Richard Balet, M.D.,[b] Lionel Larue, M.D.,[c] and Yona Barak, Ph.D.[d]

TABLE 1

Study 1: fertilization, rate of development, and blastocyst expansion in correlation to the classification of the injected motile spermatozoon.

Sperm classification	Class 1 21% (46/218)	Class 2 59% (128/218)	Class 3 20% (44/218)	Total number of spermatozoa (N = 218)
Fertilization rate	84% (39/46)[a]	73% (94/128)[a]	61% (27/44)[a]	73% (160/218)
Total blastocysts and morulae	37% (17/46)	26% (33/128)	16% (7/44)	26% (57/218)
Expanded blastocysts	15% (7/46)[b]	9% (12/128)[b]	0 (0/44)[b]	33% (19/57)

Score = Head x2 + Vacuole x3 + Base x1 = 6

Vanderzwalmen P. RBMO 2008
Setti AS. J A Rep Gen 2012
Greco E. F S 2013
Balaban B. RBMO 2011
Tanaka A. F S 2012
Knez K. Rep Bio Endoc 2011 and RBMO 2012
El Khattabi L. F S 2013

Strict morphological criteria for sperm head

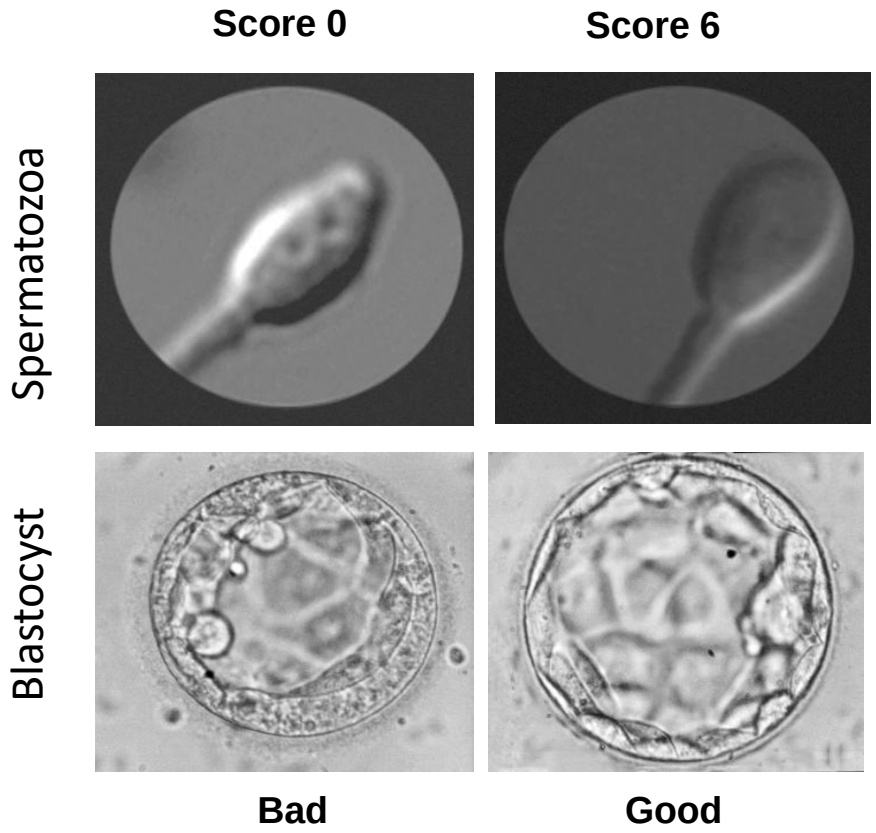

Morphological criteria are used to score spermatozoa at high magnification (6100x) and to assess expended good blastocyst quality

Cassuto et al., 2021

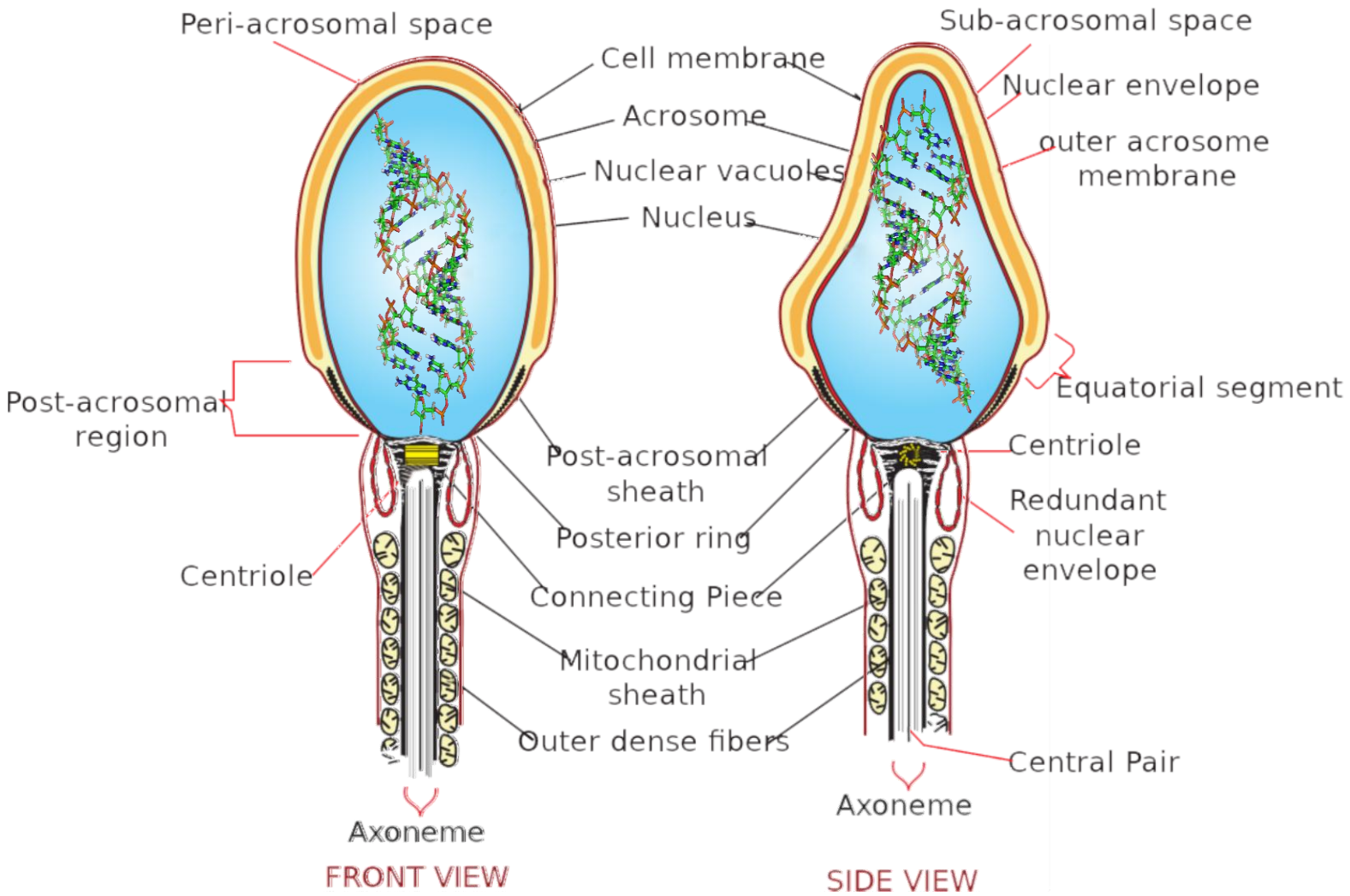
Peri-acrosomal space
Cell membrane
Acrosome
Nuclear vacuoles
Nucleus
Post-acrosomal region
Post-acrosomal sheath
Posterior ring
Centriole
Connecting Piece
Mitochondrial sheath
Outer dense fibers
Axoneme
FRONT VIEW
Sub-acrosomal space
Nuclear envelope
outer acrosome membrane
Equatorial segment
Centriole
Redundant nuclear envelope
Central Pair
Axoneme
SIDE VIEW

Different Sperm Head Morphology

Same Genetic Information
Same DNA sequences

Different Epigenetic Profiles Methylation

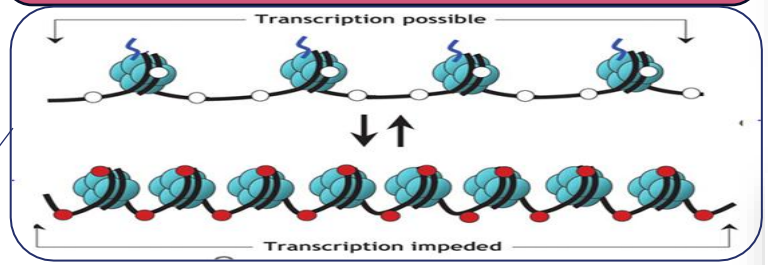

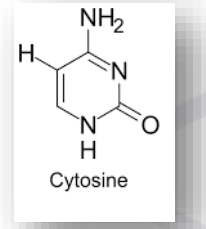

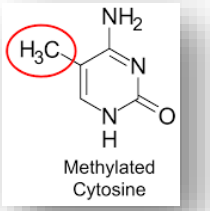

Different Outcome:

- Fertilization
- Blastocysts
- Pregnancies rate and Birth Defect

JBRA Assisted Reproduction 2021;**25**(3):466-472
doi: 10.5935/1518-0557.20210030

Original Article

Impact of Intracytoplasmic Morphologically Selected Sperm Injection (IMSI) on Birth Defects: A Systematic Review and Meta-Analysis

Felipe Dieamant[1,2], Claudia G Petersen[1,2], Laura D Vagnini[2], Adriana Renzi[2], Bruna Petersen[1,2], Fabiana Massaro[1], Camila Zamara[1], Andreia Nicoletti[1], Juliana Ricci[1], Antonio H Oliani[3], João Batista A. Oliveira[1,2], José G. Franco Jr[1,2]

May 2021

IMSI vs. ICSI: Total birth defects(structural-defects/chromosomal- abnormalities).

Total birth defects	**ICSI(n/N)**	**IMSI(n/N)**	**RR**	**95% CI**
Cassuto *et al.*,2014	22/578	6/450	0.35	0.15-0.83
Hershko-Klement *et al.*,2016	71/1394	18/498	0.71	0.43-1.17
Gaspard *et al.*,2018	26/655	8/332	0.61	0.28-1.30
Total	**119/2627**	**32/1280**	**0.60**	**0.41-0.88**

Chi^2=6.7;*P*<0.01

Cochran's Q=1.8;*P*=0.4

ESHRE - Vienna June 2019

Sperm fluorescence in situ hybridization study in nine men carrying a Robertsonian or a reciprocal translocation: relationship between segregation modes and high-magnification sperm morphology examination

Nino Guy Cassuto, M.D.,[a] *Nathalie Le Foll, M.D.,*[b] *Sandra Chantot-Bastaraud, M.D.,*[b] *Richard Balet, M.D.,*[c] *Dominique Bouret, M.D.,*[a] *Alexandre Rouen, M.D.,*[b] *Rakia Bhouri, M.D.,*[b] *Capucine Hyon, M.D.*[b] *and Jean Pierre Siffroi, M.D., Ph.D.*[b]

TABLE 3

Sperm fluorescence in situ hybridization (FISH) result… translocations carriers.

MSO				P6	P8
		…: 35	Class II: 50 Class III: 40	Class I: 25 Class II: 50 Class III: 25	Class I: 10 Class II: 60 Class III: 30	Class I: 5 Class II: 60 Class III: 35
Altern…						
NS	50%	44.40%	52.60%	47.80%	37.10%	44%
Class…	X	43.40%	53%	59.60%	23.40%	40%
Class II	43.30%	53.50%	64%	55%	35.50%	46%
Class III	50%	38.30%	41.20%	51.70%	39.10%	44.7

High-magnification in translocation carriers cannot be used to select sperm cells with a balanced chromosomal content

Chelli MH. J A Rep Gen 2013

genes April 2024 MDPI

Brief Report

Different Nuclear Architecture in Human Sperm According to Their Morphology

Nino-Guy Cassuto [1,*], Nesrine Ogal [2], Said Assou [3], Lea Ruoso [1], Eli-Jonathan Rogers [2], Miguel-José Monteiro [1], Daniel Thomas [1], Jean-Pierre Siffroi [2] and Alexandre Rouen [4,5,*]

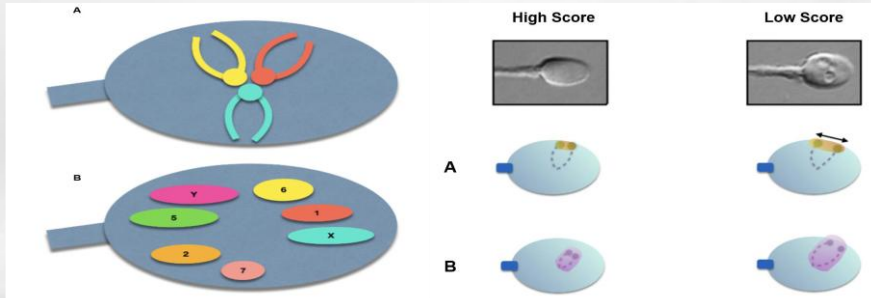

A Score 0 spermatozoa exhibit significantly higher inter-telomeric distances
B Score 0 spermatozoa exhibit significantly higher chromosomal territory areas for chromosome 1.

Table II Evaluation of sperm DNA fragmentation in large vacuole spermatozoa, isolated using MSOME.

Studies	Studied population	Large vacuole definition	Sperm DNA fragmentation analysis	Percentage of spermatozoa with fragmented DNA (mean ± s.e.m.) (%)			P	
				MSOME normal spermatozoa (*n*)	Large vacuole spermatozoa (*n*)			
Franco *et al.* (2008)	30 Infertile patients	>50% of the sperm head area	TUNEL (fixation: methanol–acetic acid)	15.9% (410)	29.1% (382)		<0.0001	
Garolla *et al.* (2008)	10 Infertile patients oligozoospermia	Not defined	TUNEL (fixation: paraformaldehyde 4%)	9.3 ± 4.8% (100)	40.1 ± 11.6% (100)		<0.001	
Wilding *et al.* (2011)	8 Infertile patients	>4% of the sperm head area	TUNEL (fixation: paraformaldehyde 4%)	6.1 ± 7.2% (331)	14.7 ± 7.2% (529)		=0.031	
Boitrelle *et al.* (2011)	15 Infertile patients	>25% of the sperm head area	TUNEL (fixation: ethanol 95%)	0.7 ± 0.4% (450)	1.3 ± 0.4% (450)		NS (=0.25)	
Perdrix *et al.* (2011)	20 Infertile patients Teratozoospermia	>13% of the sperm head area	TUNEL (fixation: methanol)	Unselected spermatozoa from native sample 11.5 ± 1.22% (10040)	14.5 ± 3.45% (560)		NS (=0.68)	
Watanabe *et al.* (2011)	10 Infertile patients 2 Sperm donors	>1.5 µm and visible at ×400 magnification	TUNEL (fixation: paraformaldehyde 4%)	3.5% (2252) 2.3% (398)	3.3% (209) 0% (18)		NS NS	
Hammoud *et al.* (2012)	8 Infertile patients with high DNA fragmentation rates >13%	>4% of the sperm head area	TUNEL (fixation: methanol–acetic acid)	4.1 ± 1.1% (191)	Anterior vacuoles 15.9 ± 2.9% (368) (a)	Posterior vacuoles 22.5 ± 3.6% (402)(b)	(a): $P = 0.013$	(b): $P = 0.0007$
				Unselected spermatozoa from native sample 26.1 ± 1.5% (8000)			(a): $P = 0.02$	(b): $P = 0.44$
Cassuto *et al.* (2012)	26 Infertile patients, Oligoasthenoteratozoospermia, Previous IVF failures	Score 0 spermatozoa (Cassuto *et al.*, 2009)	TUNEL	Unselected spermatozoa after density gradient 3.7 ± 6.7% (2600)	Score 0 4.2 ± 5.5% (2600)		NS	

Perdrix A HR 2013

Table I Evaluation of sperm chromatin compaction in large vacuole spermatozoa, isolated using MSOME.

Studies	Studied population	Definition of large vacuoles	Sperm chromatin compaction analysis	Abnormal sperm chromatin compaction (mean ± s.e.m.) (%)		P
				MSOME normal spermatozoa (*n*)	Large vacuole spermatozoa (*n*)	
Franco *et al.* (2008)	30 Infertile patients	>50% of the sperm head area	CMA3		67.9% (371)	<0.000
Garolla *et al.* (2008)	10 Infertile patients, oligozoospermia				71.9 ± 11.1% (100)	<0.001
Boitrelle *et al.* (2011)	15 Infertile patients				36.2 ± 1.9% (450)	<0.000
Perdrix *et al.* (2011)	20 Infertile patients Teratozoospermia		Aniline blue	Unselected spermatozoa from native sample 26.5 ± 2.57% (9980)	50.4 ± 3.1% (460)	<0.000
Cassuto *et al.* (2012)	26 Infertile patients oligoasthenoteratozoospermia Previous IVF failures	Score 0 spermatozoa (Cassuto *et al.*, 2009)	Aniline blue	Unselected spermatozoa after density gradient 10.1 ± 6.0% (2600)	19.5 ± 8.7% (2600)	<0.000
Franco *et al.* (2012)	66 Infertile patients	>50% of sperm head area	CMA3	40.3% (835)	53.2% (1351)	<0.000

Failure of Chromatin Condensation

Perdrix A HR 2013

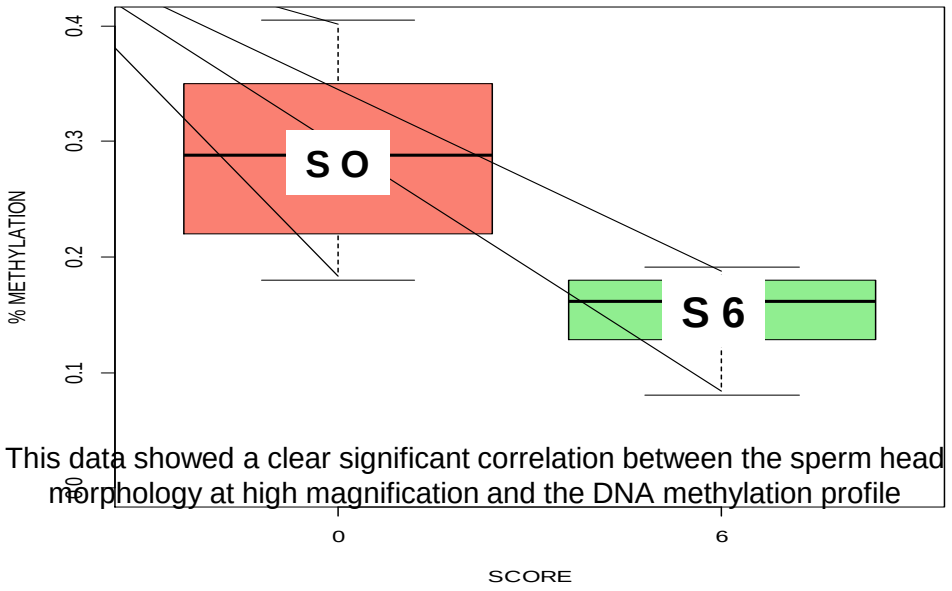

This data showed a clear significant correlation between the sperm head morphology at high magnification and the DNA methylation profile

Genome-wide microRNA expression profiling in human spermatozoa and its relation to sperm quality

NG. CASSUTO [1], L. RUOSO [1], G. KEROMNES [2], L. PRAT-ELLENBERG [3], N. LEDEE [4], C. CHAO [5], H. MOUIK [6], S. ASSOU [7]

GCAT TACG GCAT genes

MDPI

Published: 4 January 2025

Article

Genome-Wide microRNA Expression Profiling in Human Spermatozoa and Its Relation to Sperm Quality

Nino-Guy Cassuto [1,*], Florence Boitrelle [2], Hakima Mouik [3], Lionel Larue [4], Gwenola Keromnes [4], Nathalie Lédée [5], Laura Part-Ellenberg [6], Geraldine Dray [6], Léa Ruoso [1], Alexandre Rouen [7], John De Vos [8] and Said Assou [8,*]

➤ Background

We previously int
spermatozoa, whe
This is characterize
extrusion or invag
normal base. Suc
blastocyst stage. C
abnormalities, an
categorizing them
(miRNA) profiles
versus score 0) an

➤ Experimental

We used a
microarray
analyze the
profile (Score 6
0). We only
miRNA profiles
a Fold change>
value ≤ 0.05.

➤ Differences in

(A) Principal Component Analysis (PCA) in 3-dimensional plots represents the different miRNA expression patterns from the 10 samples. Two distinct groups were obtained based on their miRNA expression profiles. (B) The dendrogram shows that the 5 samples S6 clustered in 1 Red branch. The 5 samples S0 samples in 1 Blue branch.

(A) Violin plot comparing the top ten microRNAs that are differently expressed in Score 6 (n = 5) and Score 0 samples (n = 5). (B) The heat map showed a molecular signature based on the 10 selected microRNAs upregulated in S6 Vs. S0.

ownregulated

MAP2

NAs revealed that key
such as *PDGFA* and
8 and miR-92a. The
ssues using RNA-seq
Expression repository
sed in testis tissue

rm quality
ydative stress

The key miRNAs overexpressed in Score 6 are predicted to target messenger RNA involved in biological functions of the spermatozoa, mTOR signaling, and oxydative stress.

➤ Conclusions

The profiling of miRNAs repertoire in scored spermatozoa morphology opens new perspectives to explore male fertility status and provides a biomarker panel for sperm analysis during the ART procedure.

Morphology and Gene expression

PLoS One. 2019 Mar 21;14(3):e0214275. doi: 10.1371/journal.pone.0214275. eCollection 2019.

Genetic and epigenetic profiling of the infertile male

Stephanie Cheung [1], Alessandra Parrella [1], Zev Rosenwaks [1], Gianpiero D Palermo [1]

Research Article | Open Access

Volume 2021 | Article ID 1434546 | https://doi.org/10.1155/2021/1434546

Show citation

Hindawi

Molecular Profiling of Spermatozoa Reveals Correlations between Morphology and Gene Expression: A Novel Biomarker Panel for Male Infertility

Nino Guy Cassuto, [1] David Piquemal, [2] Florence Boitrelle, [3,4] Lionel Larue, [5] Nathalie Lédée, [6] Ghada Hatem, [7] Léa Ruoso, [1] Dominique Bouret, [1] Jean-Pierre Siffroi, [8] Alexandre Rouen, [8] and Said Assou [9]

Study Design

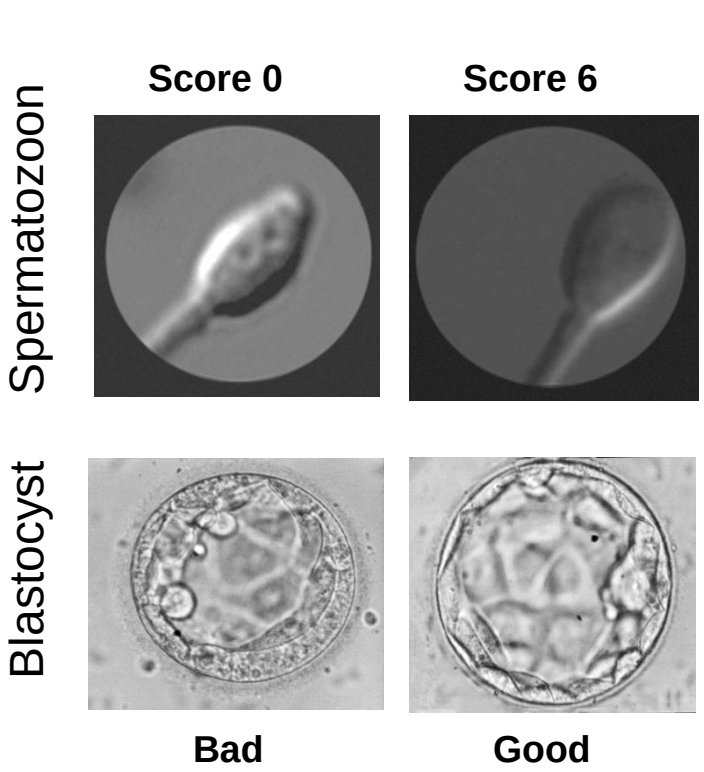

Sample set A

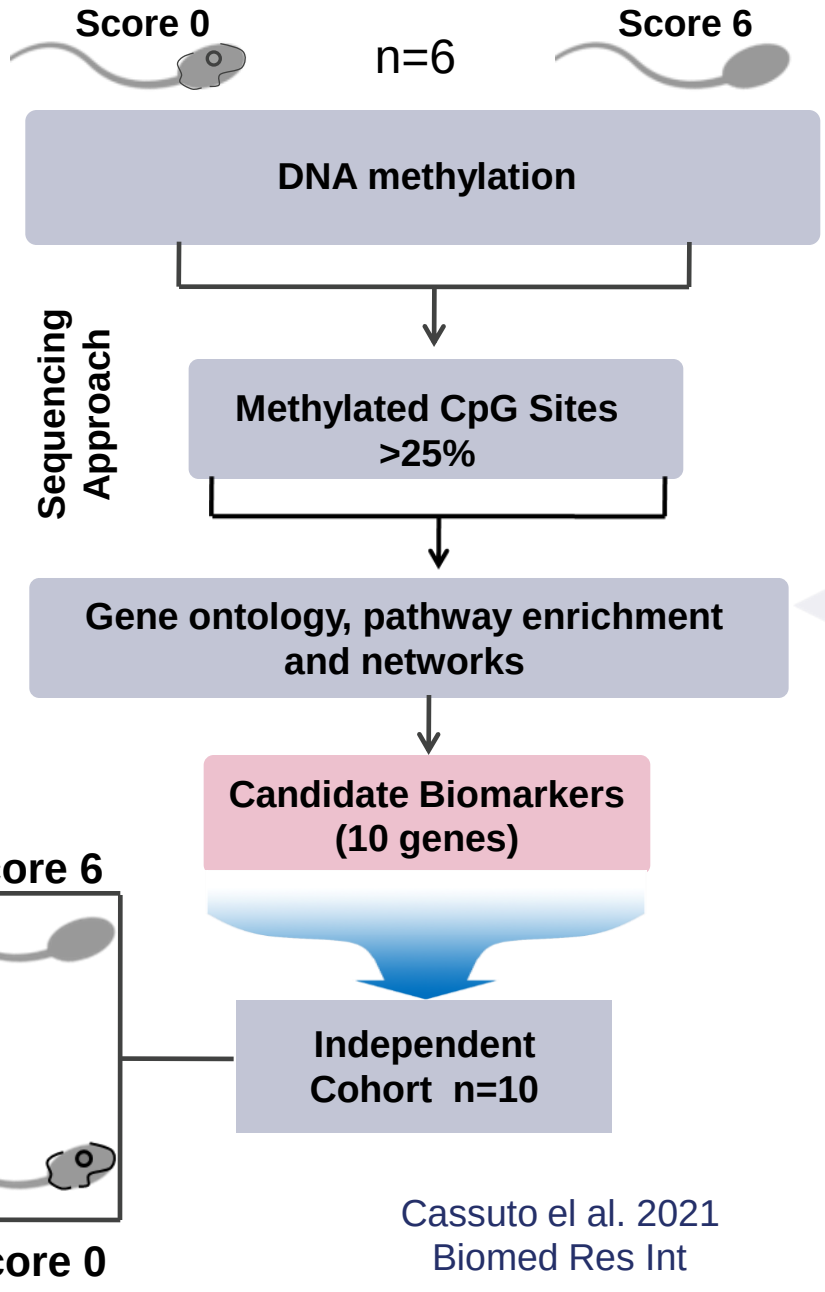

Cassuto el al. 2021
Biomed Res Int

Top-ranked functional protein interaction network

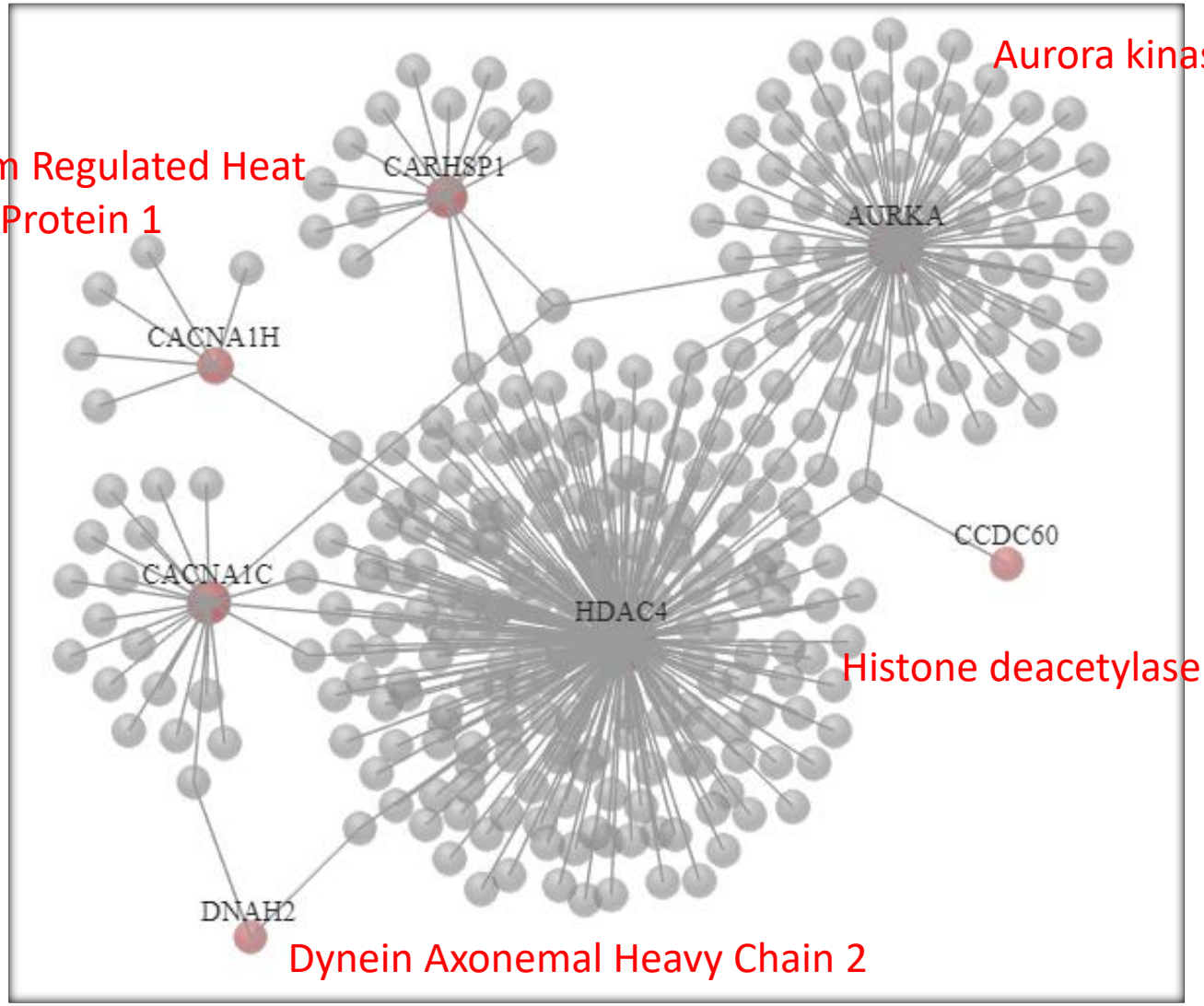

Calcium Regulated Heat Stable Protein 1

Aurora kinase A

Histone deacetylase 4

Dynein Axonemal Heavy Chain 2

CFAP46 Cilia And Flagella Associated Protein 46

Artificial Intelligence and Subjectivity

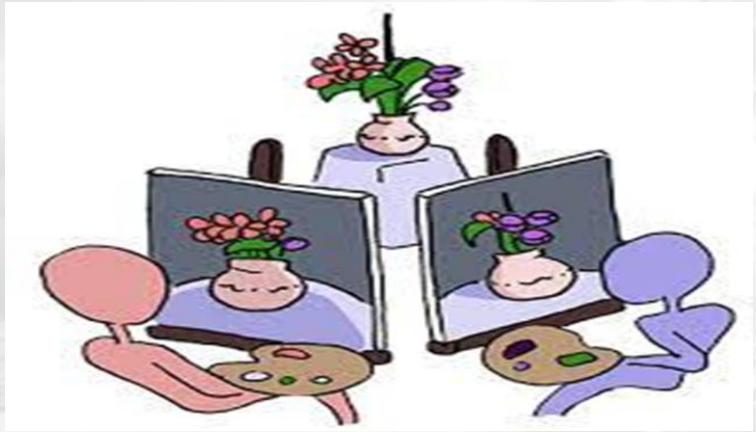

WHAT INFLUENCES SUBJECTIVITY ???

All data we generate remains stored and used for a decision
no operator-dependent

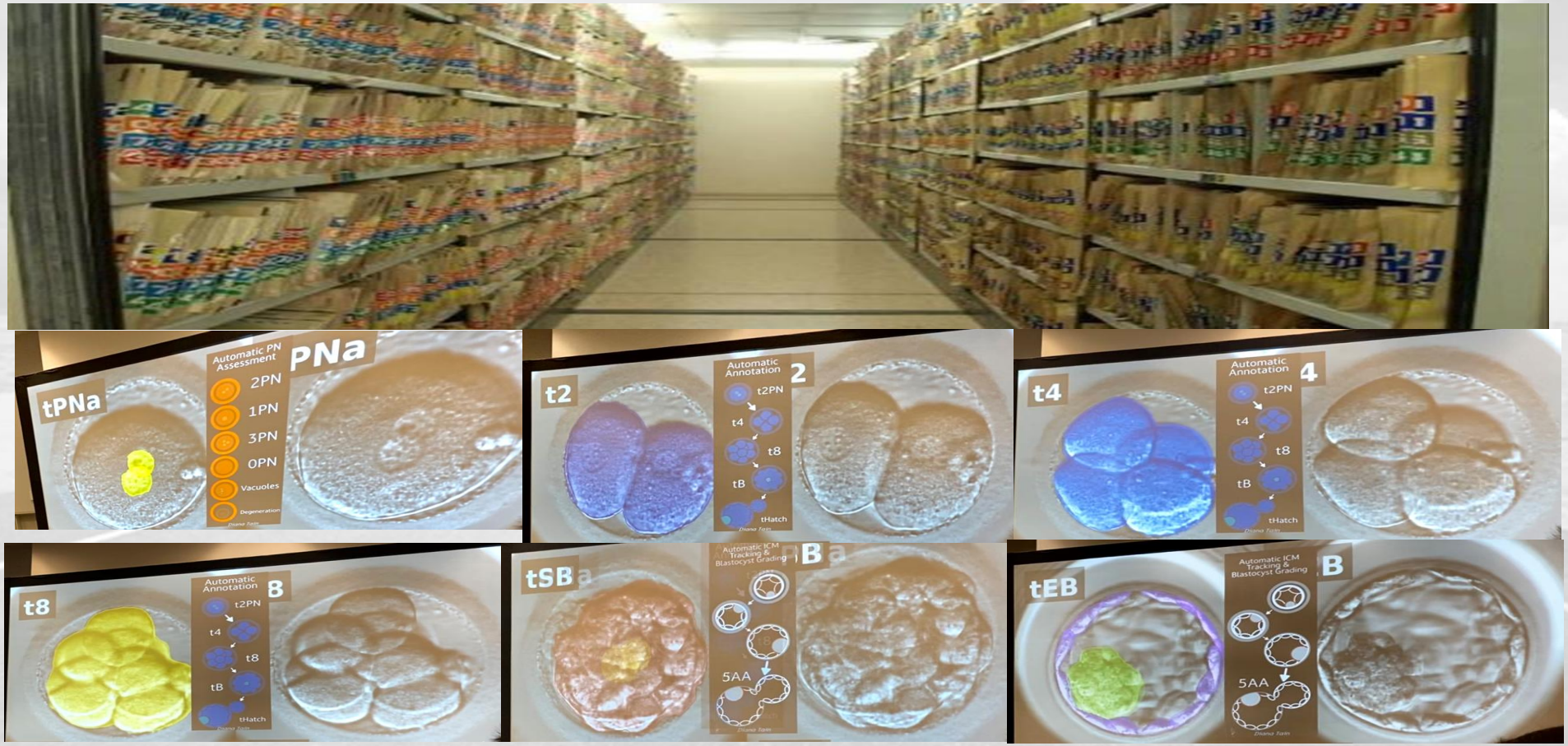

What’s AI Technology ?

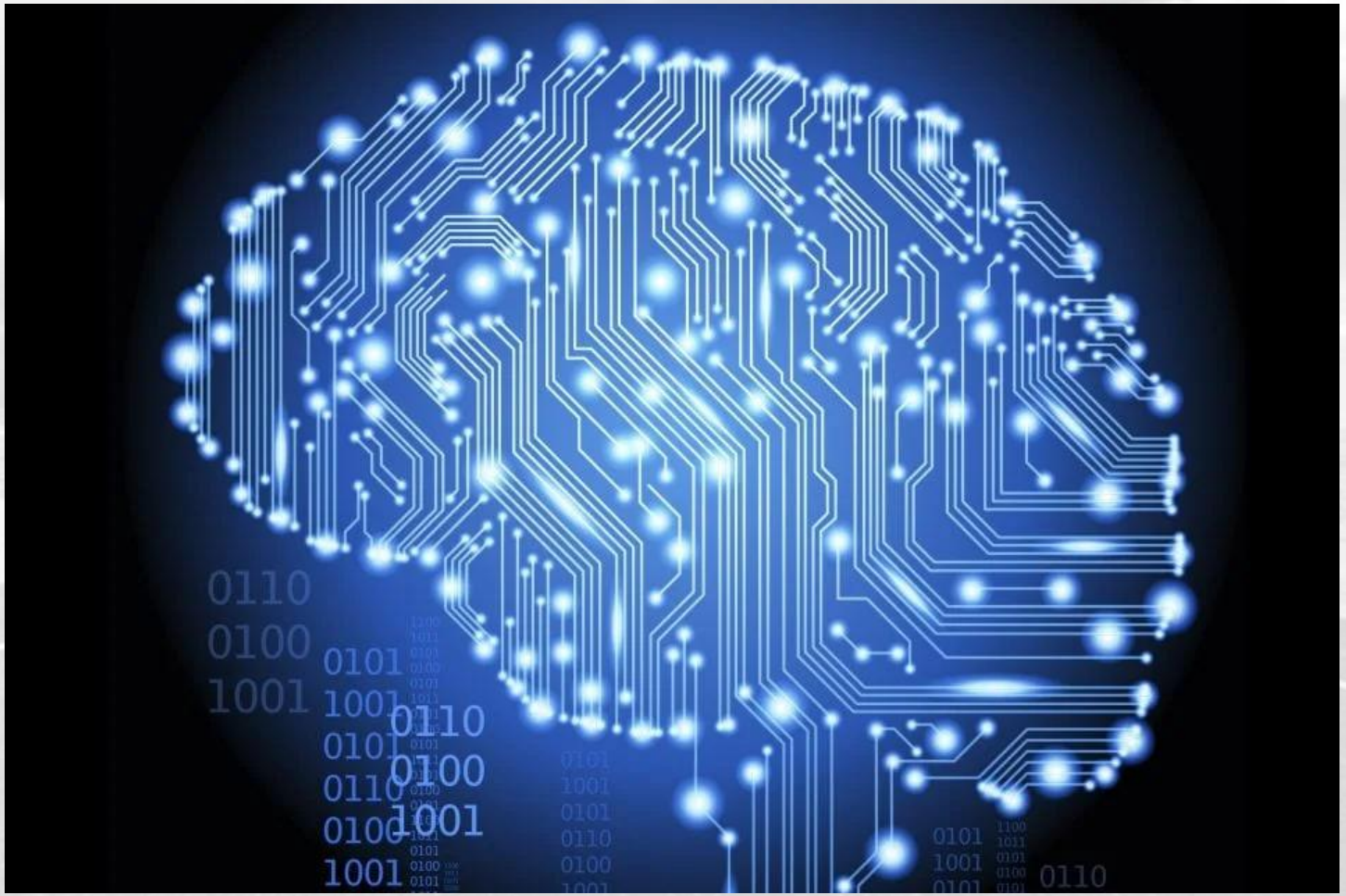

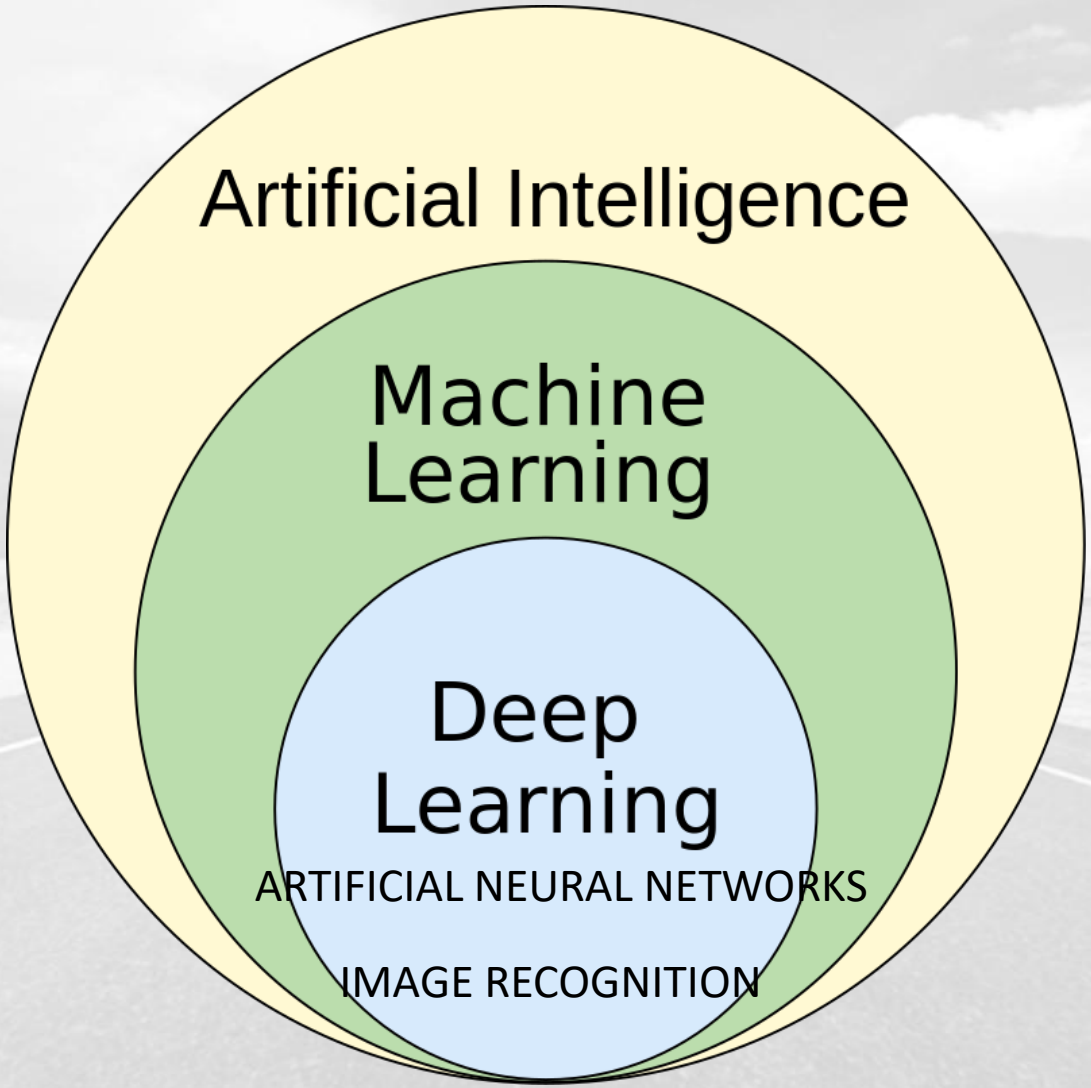
Artificial Intelligence
Machine Learning
Deep Learning
ARTIFICIAL NEURAL NETWORKS
IMAGE RECOGNITION

AI needs huge data! It's a hungry giant!!!

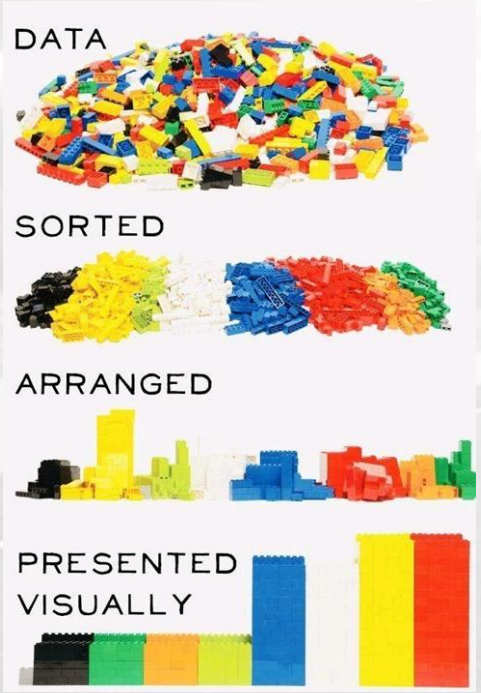

Data: 800 hours of videos:
More than 3 months in continued vision

Sorted:15 000 frames were randomly captured

Arranged: by embryologist experts labeling and classified

Presented visually on the screen
Machine learning / Deep learning
Teach the machine to do the job

AI Modules

- Cell Detection
- Cell Morphology Classification
- Cell 3D Tracking & Motion Estimation

Standalone application:

1. During runtime, the AI modules apply mathematical operations to the input matrices.
2. The output is a probability vector.
3. The mathematical operations are learnt during system development
4. Annotated datasets are utilized for learning.

Algorithms Block Diagram

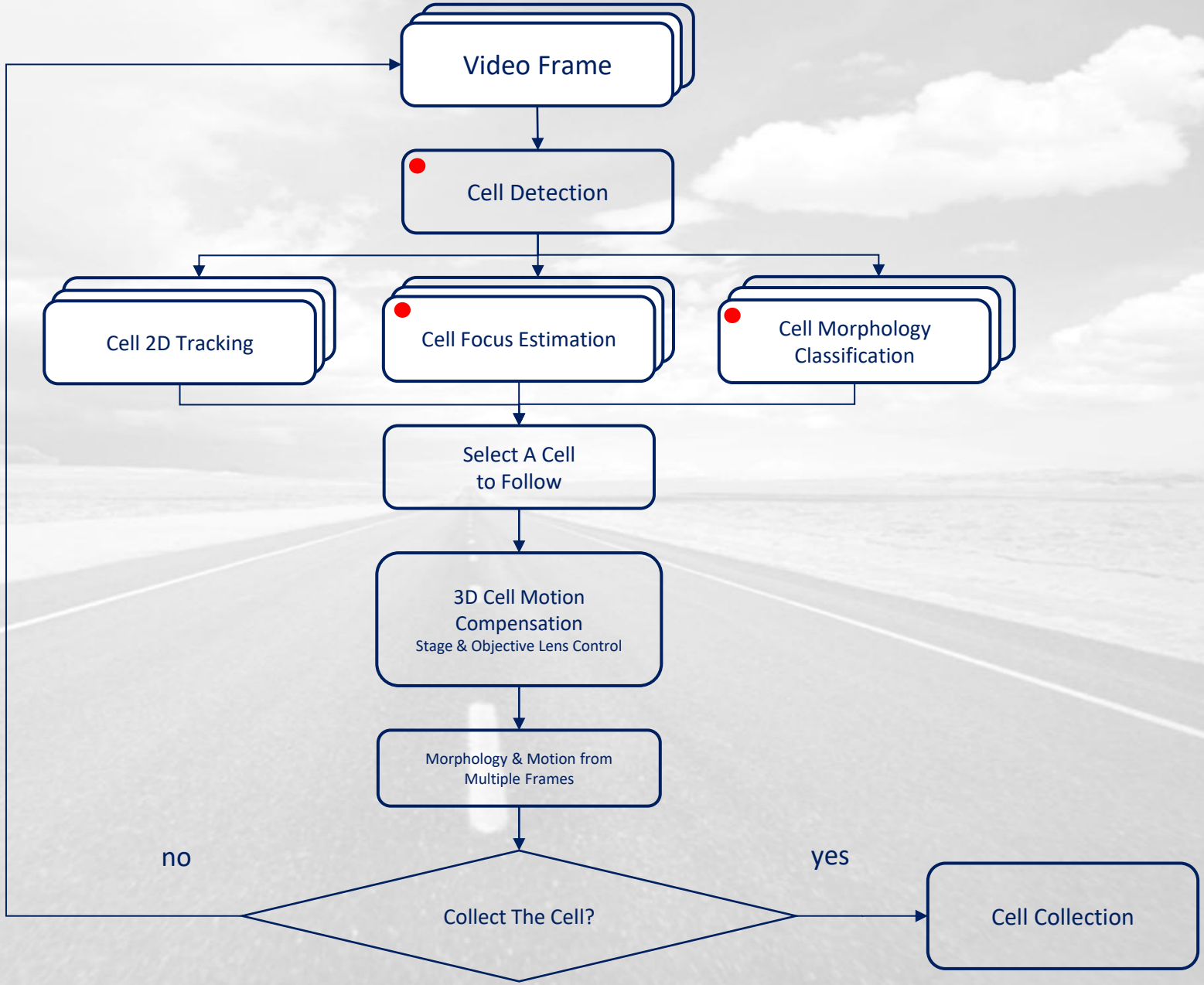

● = AI Module

1 - AI Module

- **Cell Detection: AI**
  - Input: a video frame 30 frames /Seconds
  - Output: a list of cell-bounding boxes
  - θ = neural network parameters [1]

SPZ à 1600 px/µm : 38.4 MP
SPZ à 6100 px/µm : 558.15 MP

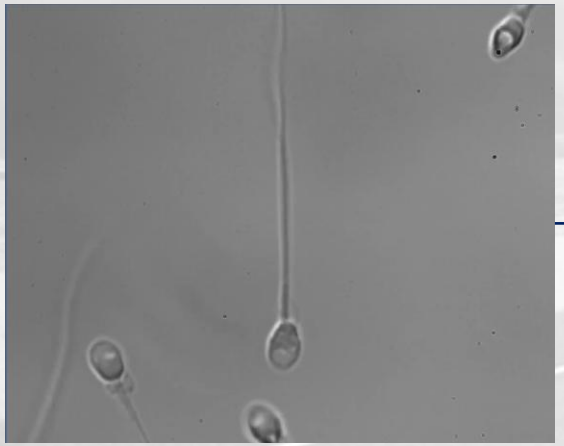

Deep Neural Network, θ

x^3	y	Width	Height	Probability[3]
0.20	0.80	0.10	0.20	0.9
0.45	0.95	0.15	0.10	0.88
0.50	0.75	0.08	0.25	0.81
0.92	0.05	0.10	0.12	0.73
0.42	0.56	0.21	0.07	0.60
⋮	⋮	⋮	⋮	⋮
0.89	0.19	0.26	0.22	0.41

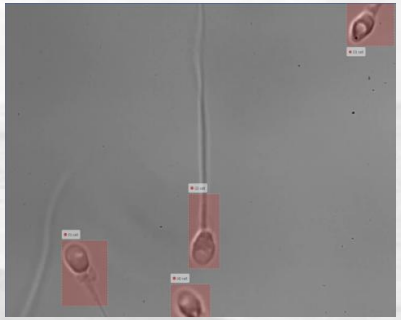

Input: video frame (a matrix)

Output: tabulated data (a matrix)

Bounding box overlay

[1] θ = parameters that describe the mathematical operation applied to the input image; these parameters are optimized as to minimize the detection error with respect to manually-annotated images.
[2] values are relative to the image width and height.
[3] a threshold probability value allows one to exclude non-cell bounding boxes.

2 - AI Module

- **Cell Morphology Classification**
  - Input: a cell bounding-box image[1]
  - Output: probability vector (normal, abnormal)
  - θ = neural network parameters

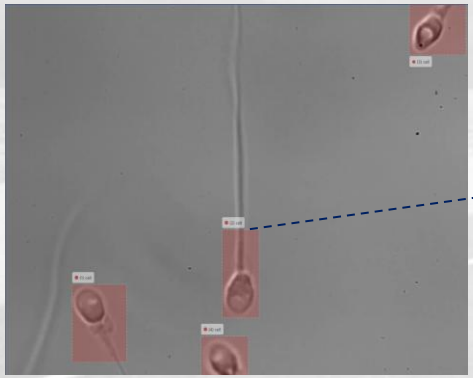

Input: cell image (a matrix)

Deep Neural Network, θ

$(p, 1-p)$

Output:argmax over the probability vector (normal, abnormal)

[1] All cell bounding-box images undergo morphology classification.

3 - AI Module

- Cell 3D Tracking & Motion Estimation
  - Lateral Direction (not AI):
    - Input: a sequence of detection results
    - Output: a sequence of cell trajectories
    - Autoregressive motion model

Input:
detection results of
consecutive frames

x	y	Width	Height	Probability
0.20	0.80	0.10	0.20	0.9
0.45	0.95	0.15	0.10	0.88
0.50	0.75	0.08	0.25	0.81
0.92	0.05	0.10	0.12	0.73

x	y	Width	Height	Probability
0.43	0.90	0.13	0.10	0.92
0.25	0.77	0.18	0.22	0.83
0.51	0.69	0.12	0.25	0.81
0.90	0.08	0.11	0.15	0.73

frame *n* Frame *n*+1

Output: cell tracks
Track 1 (*x*,*y*) = (0.2,0.80) ⇢ (0.25, 0.77) ⇢
Track 2 (*x*,*y*) = (0.45, 0.95) ⇢ (0.43, 0.90) ⇢
Track 3 (*x*,*y*) = (0.50, 0.75) ⇢ (0.51, 0.69) ⇢
Track4 (*x*,*y*) = (0.92, 0.05) ⇢ (0.90, 0.08) ⇢

- **Axial direction, Focus: AI**
  - Input: image of a cell
  - Output: a probability vector
  - θ = neural network parameters

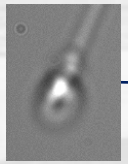

Deep Neural Network, θ

(p, q, r)
p = probability of being below focus plane
q = probability of being in focus
$r = 1 - p - q$ = probability of being above focus

Input:cell image
(e.g., below focus)

Output:argmax over the probability vector

- Selected Cell:
  - Stage x-y position:
    - can compensate for cell lateral movement
    - can keep the cell at the center of the field of view.
  - Objective lens z-position:
    can correct for defocus situations that originate from the axial motion of the cell.

- Motion estimation from track information over multiple frames.
- Morphology classification from majority vote of multiple frames.

AI Modules

- AI learning is based on
  - Datasets with ground truth annotations
  - neural network architectures
  - numerical optimization of loss functions
  - performance analysis & generalization safeguards to unseen data.

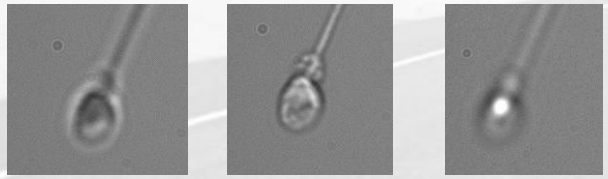

above focus | at focus | below focus

Cell Focus Dataset Exemplar

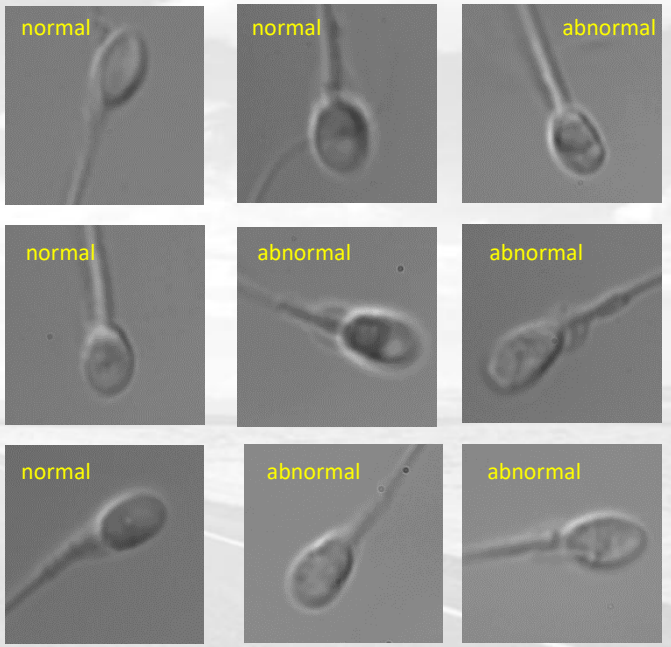

Cell Classification Dataset Exemplar

How It Works – AI Classification

AI classifies sperm cells' morphology at high magnification

- **Proprietary algorithm processes** the video stream of "live" sperm in real time
- **Autonomously classifies sperm** cells based on their morphology & motility at high-magnification (×6,100) **30 frames /Seconds**
- **Proprietary BAIBYS' algorithm controls** the motorized X-Y stage in real time to maintain the selected sperm cell in the middle of the field of view to allow reviewing the cell from all sides

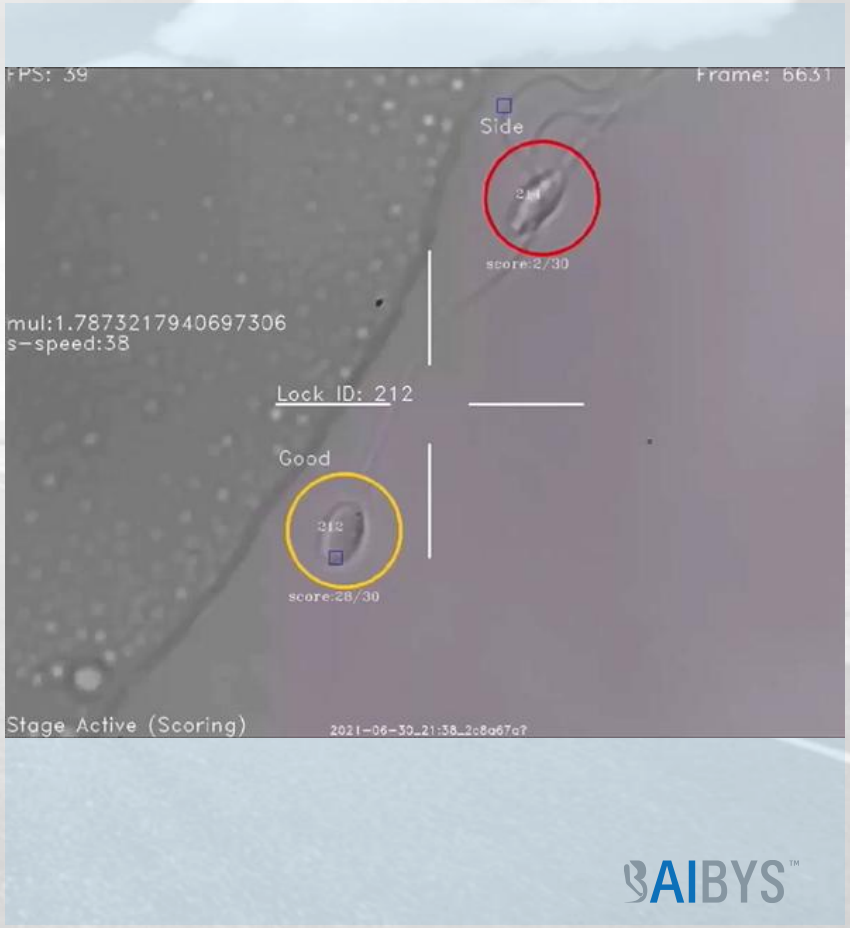

BAIBYS™

HOW IT’S WORK

Control Panel of the system and Codes for all the system generated by AI


Gradient Focus: 29.26
Contrast Focus: 311.05
Current Z: 0.00
Side
Lock ID: 1086
Side
Blue
Unk
Ceil

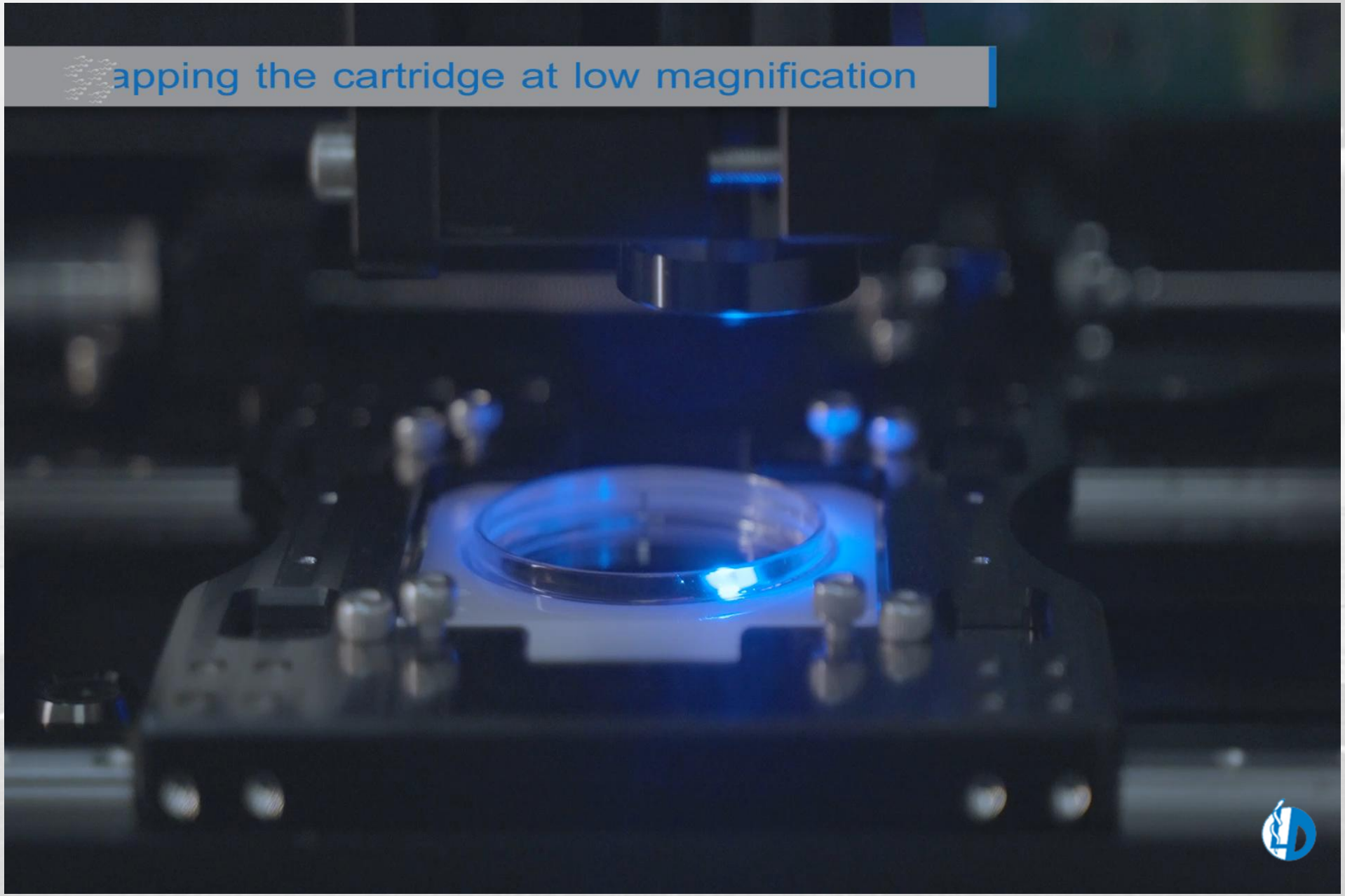
apping the cartridge at low magnification

Conclusions

- ☑ Morphology is correlated with the DNA quality;
- ☑ Sperm selection before ICSI is a crucial step;

  because we are at the beginning of the process.
- ☑ Autonomous sperm selection system;

  based on DNA quality and epigenetic profiles.
- ☑ Using AI combined with Micro Robotic.

MERCI